A General Modeling for Key Performance Indicators Optimization in Two-Tier Heterogeneous Networks

Vincent Savaux* and Pape Abdoulaye Fam

b-com, Rennes, France

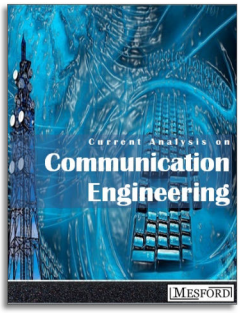

Abstract:

This paper deals with the mathematical modeling of two-tier heterogeneous networks (HetNets) through measure theory, and the optimization of the related key performance indicators (KPIs). Thus, any HetNet can be described as a σ—algebra, on which measures can be defined. As a result, we make a connection between the mathematical and the physical features of the KPIs of HetNets, such as the capacity or the energy efficiency (EE), which are extensive and intensive performance metrics, respectively. Then, it is shown that the extensive property remains in presence of inter-cell interferences. Through examples, we highlight that the optimization of extensive variables is more simple than the optimization of intensive variables, since extensive variables are often concave/convex functions of their parameters. Finally, the mathematical modeling of HetNets is illustrated through applications and examples, such as the maximization of the capacity in a long term evolution (LTE) macrocell/femtocell HetNet, as well as the minimization of the power consumption in a broadcast/unicast hybrid network.

Publication History: Received: 12 August 2018 | Revised: 19 September 2018 |Accepted: 27 September 2018

Keywords:
Heterogeneous network, Key performance indicator, Measure, Optimization, LTE, Broadcast, Capacity, Energy efficiency

1. INTRODUCTION

Heterogeneous network (HetNet) could be a sustainable solution for next generations of communications systems in order to face the increasing data rate demand while limiting the power consumption. As a matter of fact, long term evolution-(LTE-) advanced releases already include the heterogeneous deployments of picocells and femtocells within the macrocells [1,2]. More generally, HetNets shall involve different technologies and standards, such as LTE/WiFi [3], or broadcast/unicast [4] hybrid network.

The aim of HetNets is to ensure the users access to multimedia contents while reducing the power consumption of the base stations. In fact, the increase of the number of low power services access points and hotspots within macrocells limits the congestion of the network, and leads to a more reliable coverage area, in particular in urban areas. For broadcast/unicast hybrid network (e.g. digital video broadcasting (DVB)/LTE), the principle is to broadcast the most popular multimedia contents in order to limit the use of the LTE base transceiver stations BTSs. HetNets, and networks in general, are usually characterized and compared by using key performance indicators such as the capacity, i.e. the achievable throughput per user equipment (UE), the power consumption of the BTSs, and the energy efficiency, which can be defined as the ratio of the capacity to the power consumption.

Literature on optimization of wireless networks and HetNets is very extensive. However, most of the papers focus on one of the KPIs, and deal with the optimization of this particular metric. Thus, authors of [5-8] propose an optimization of the HetNets with respect to the capacity, whereas in [9-12] the standpoint of the EE has been chosen. Alternatively, Lin *et al.* propose in [13] an optimization of macro-femtocells HetNets from a business point of view, where the revenue is maximized in function of the deployed femtocells.

In this paper, we propose to model any two-tier HetNet thanks to the measure theory. Thus, it is shown that the BTSs and UEs of the network can generate a σ—algebra, on which a measure can be defined. Furthermore we make the association between the physical and the mathematical natures of the KPIs. More precisely, a KPI that can be defined as a mathematical measure is an extensive variable, whereas a KPI that cannot be defined as a measure is an intensive variable. In

*Address correspondence to this author at the 1219 avenue des champs blancs Postal Code:35510, Cesson-Sévigné, Rennes France.
E-mail: vincent.savaux@b-com.com

Mesford Publisher Inc
Office Address: Suite 2205, 350 Webb Drive, Mississauga, ON L5B3W4, Canada; T: +1 (647) 7109849 |E: cace@mesford.ca, contact@mesford.ca, https://mesford.ca/journals/cace/

addition, we provide a general expression of the KPIs optimization problem, and we deduce that the optimization of extensive KPIs may be reduced to simple problem since measures can be summed, especially as the metrics are concave or convex functions. The proposed mathematical model is supported and illustrated through two examples : the maximization of the capacity in LTE macro- cell/femtocell HetNet and the minimization of the power consumption in broadcast/unicast hybrid.

The remainder of this paper is organized as follows: Section 2 is a reminder concerning the KPIs of HetNets such as the capacity, the power consumption, and the energy efficiency. In Section 3, we derive the general mathematical model of the two-tier HetNets, then we describe different applications in Sections 4 and 5. Section 6 is devoted to the simulations results, and we conclude in Section 7.

2. KEY PERFORMANCE INDICATORS

2.1. Ergodic Capacity

According to [14,15], the ergodic (or Shannon) capacity (in bits/s), when no channel state information (CSI) is available at the transmitter, can be expressed as

$$C = E_{B,\gamma}\{B\log_2(1+\gamma)\}, \tag{1}$$

where $E_{a,b}\{.\}$ is the mathematical expectation according to variables a and b, B is the allocated bandwidth, and γ is the signal-to-noise ratio (SNR). Since it can be reasonably assumed that the allocated bandwidth is independent of the SNR, it is usual to rewrite (1) as

$$C = E\{B\}\int_0^{+\infty}\log_2(1+\gamma)f_\gamma(\gamma)\mathrm{d}\gamma, \tag{2}$$

where f_γ is the distribution of the SNR. In Rayleigh channel, the SNR is given by the exponential distribution:

$$f_\gamma(\gamma) = \frac{1}{2\bar{\gamma}}\exp\left(-\frac{\gamma}{2\bar{\gamma}}\right), \tag{3}$$

where $\bar{\gamma}$ is the average SNR value. Other models as Nakagami (for the multipath fading), log-normal (for the shadowing), and a composite multipath/shadowing are provided in [16]. Note that less complex alternatives to these general models have been recently proposed. Thus, authors of [17] approximated the log-normal shadowing by the inverse-Gaussian shadowing, and the authors of [18] model the multipath/shadowing channel by a mixture of Gaussian distributions. The average bandwidth E{B}, for its part, depends on the transmission type (related to the transmission standard), as well as the implemented scheduler. For instance, in LTE using round robin scheduler, the average bandwidth could be expressed as $E\{B\} = N_{RB}B_{RB}$, with N_{RB} average allocated resource blocks (RBs), and B_{RB} the bandwidth of a RB. In WiFi using carrier sense multiple access with collision avoidance (CSMA-CA), the average bandwidth could be expressed as $E\{B\} = pB$ where p is the probability to access the medium.

2.2. Spectral and Energy Efficiency

The spectral efficiency (SE) is defined as the ratio of the capacity to the allocated bandwidth, and it is usually given in bps/Hz (bits per second per Hertz) by:

$$SE = \frac{C}{E\{B\}}. \tag{4}$$

The physical difference between the capacity and the SE is that the capacity is an extensive variable, whereas the SE is an intensive variable. Extensive and intensive variables can be defined as follows.

Definition 1. Intensive/extensive variable. An intensive variable is independent of the size of the system to which it is related, whereas an extensive variable is proportional to the size of the system.

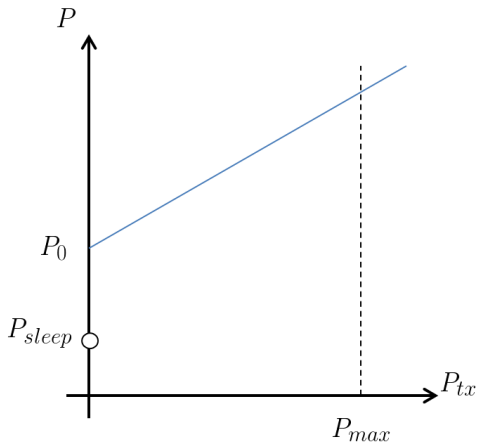

Figure 1: Load-dependent power consumption model from [19]

Table 1: Power consumption parameters extracted from [19,20]

BS type	P_{max} [W]	Δ_p	P_0 [W]	P_{sleep} [W]
LPLT: Macro	40	4.75	260	150
LPLT: Femto	1	1.5	96.2	62
HPHT: Broadcast	10^6	6	2.6×10^3	150

As a consequence of the above definition, the SE metric allows to make a fair comparison between systems of different nature and size, unlike the capacity metric. In fact, two LTE systems with the same transmission mode but two different bandwidths, e.g. 10 and 20 MHz, lead to different capacity values (the 20 MHz bandwidth achieves twice the capacity of the 10 MHz bandwidth), but have the same SE.

The energy efficiency (EE), given in bps/J (or equivalently in bps/Hz/W), is a KPI which makes the link between the SE and the power consumption, and it is defined by

$$EE = \frac{C}{E\{B\}P}, \tag{5}$$

where P is the average power consumption needed for a reliable transmission. According to the chosen model, the power P may refer to the average power which is required to transmit at a given data rate [21], the radiated power which is linked to the transmit power in [22], or the total consumed power by both transmitter and receiver devices such as in [23]. As indicated in [20], [24], base stations represent a dominant share of the total power consumption in mobile broadband and broadcast networks. In order to evaluate the power consumption of the base stations, a simple and accurate power model is proposed in [20]. The proposed power model is based on a combination of the power consumption of base station components and sub-components such as analog Radio Frequency (RF), baseband (BB) processing, and power amplifier and the power system (cooling). As shown in Fig. 1, the power consumption P of a base station can be obtained from the following function [19]

$$P = \begin{cases} P_0 + \Delta_p P_{max} \rho & \text{if base station is turned ON} \\ P_{sleep} & \text{otherwise} \end{cases}, \quad (6)$$

where P_0 is the power consumption at the non-zero output power, P_{max} is the transmission power per carrier, P_{sleep} is the power consumption in sleep mode, Δ_p is the slope of the load-dependent power model and depends on the type of the base station, and ρ is the ratio of the used number of carriers to the total number of carriers. Table 1 shows power consumption model parameters for different types of base station. The power consumption KPI is very relevant in 4G/5G networks which aim to offer a higher capacity at a lower power consumption.

3. MATHEMATICAL MODELING AND OPTIMIZATION OF HET- NETS

This section aims to model any HetNet by using the concept of measure in mathematics to provide a general expression of the KPIs optimization problem. Furthermore the proposed modeling highlights the connection between the mathematical feature and the physical feature of the KPIs, which leads to a reduction of the complexity of the KPIs optimization problem.

3.1. Mathematical Modeling of the Heterogeneous Network

Let us consider a HetNet composed of two technologies, namely two sizes of cells (e.g. macrocell/femtocell). Furthermore, it is assumed that any UEs can only be connected to one of the cells at the same time. Since the BTSs of the HetNet are also independent, we can define the HetNet as a set S of elements (namely BTSs and UEs) such that:

$$S = S_1 \cup S_2, \quad (7)$$

where Si, $i \in \{1,2\}$ is the subset of the HetNet S which contains the BTSs (in the set Bi) corresponding to the i-th technology, as well as the UEs (in the set Ui) which are connected to those BTSs, i.e.

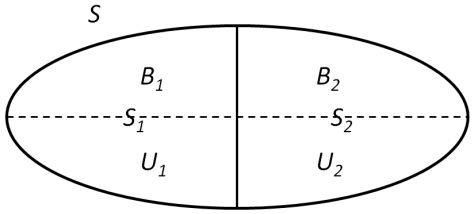

Figure 2: HetNet defined as an union of subsets.

$$S_i = B_i \cup U_i, \text{ with}$$
$$B_i = \{BTS_{1,i}, BTS_{2,i}, ..., BTS_{B_i|,i}\}$$
$$U_i = \{UE_{1,i}, UE_{2,i}, ..., UE_{U_i|,i}\},$$

where $|Bi|$ and $|Ui|$ are the cardinalities of the sets Bi and Ui, respectively. According to the previous assumptions, we trivially have $S_1 \cap S_2 = \emptyset$, $B_i \cap U_i = \emptyset$. Thus the HetNet can be simply described as in Fig. 2, where Si and $S2$ are separated by a solid line. Note that the size of the area in Fig. 2 may not correspond to the cardinalities of the different subsets.

Based on the previous considerations, we can build the σ-algebra on S denoted by Σ and generated by $\Sigma = \sigma(\{B_1, B_2, U_1, U_2\})$, in such a way that (S,Σ) is a measurable space. It can be straightforwardly verified that

- The power consumption P and the capacity C are two measures on Σ in the mathematical sense. In fact, for any $X \in \Sigma$ they satisfy the three following properties (considering for P instance):
  1. $P(X) \geq 0$ (non-negativity),
  2. $P(\emptyset) = 0$ (null empty set),
  3. $P\left(\sum_k X_k\right) = \sum_k P(X_k)$ (σ-additivity).
- The SE and the EE are not measures in the mathematical sense. In fact, they are defined as the ratio of two measures, and therefore they cannot be measures themselves (only the addition of two measures is a measure).

It is worth noticing that we can make the association between the previous mathematical representation and the physical one stated in Section 2.2:

Proposition 1. A KPI that can be defined as a (mathematical) measure is an extensive variable, whereas a KPI that is not a measure is an intensive variable.

3.2. Discussion on the Mathematical Modeling

The capacity modeling presented above is simplified, as no inter-cell interferences has been considered. We hereby extend (generalize) the developments to a more practical case where interferences are taken into account in the model. Then, we discuss the conditions where Proposition 1 holds or not.

Let us consider a network composed of N_{BTS} BTSs, such that the density ρ of antennas per unit of area is constant, namely $\rho = N_{BTS}/\mathcal{A}$, where $\mathcal{A}$ is the area where the antennas are deployed. In presence of inter-cell interferences, the overall capacity in the whole network can be expressed as

$$C = E_{B,\gamma_I}\{N_{BTS} B \log_2(1+\gamma_I)\}, \quad (8)$$

where γ_I is the signal-to-noise plus interference ratio (SINR), which can be written as

$$\gamma_I = \frac{GP}{P_I + P_W}. \quad (9)$$

In (9), G represents the channel gain, including shadowing and fast fading, P_W is the noise power, and P_I is the interference power. The latter can be defined as a function of the $N_{BTS} - 1$ interfering BTSs by using a general propagation model (see [16] for instance) as follows:

$$\begin{aligned} P_I &= f(N_{BTS}-1, P) \\ &= \sum_{i=1}^{N_{BTS}-1} P_i \\ &= \sum_{i=1}^{N_{BTS}} {}^{1} G_i P_r \left(\frac{r_i}{r_0}\right)^{\alpha}, \end{aligned} \quad (10)$$

where P_i is the interference power from the i-th BTS, G_i is the corresponding channel gain, P_r is the transmit power measured at an arbitrary distance r_0[1] , r_i is the distance to the interfering BTS, and α is the path-loss exponent. It appears that the capacity C in (8) is not a measure nor a extensive quantity with respect to N_{BTS}, since C is not proportional to N_{BTS}. However, it can be shown that the capacity in (8) is indeed an extensive variable with respect to N_{BTS} based on the *thermodynamic limit* condition [25], i.e. when N_{BTS} is large. In fact, if the density ρ is fixed, then it can be shown that the interference power is upper bounded as:

$$\lim_{N_{BTS}\to+\infty} P_I = P_I^M < +\infty. \quad (11)$$

The result in (11) may be intuitive, as it is known that the interfering BTSs are close to cell of interest. In fact, any additional BTS which is deployed far from the cell of interest induces negligible interferences. However, this result is mathematically proved in Appendix A. It is known from the principle of *thermodynamic limit* [25] that the capacity in (8) is an extensive quantity with respect to N_{BTS} if

$$\lim_{N_{BTS}\to+\infty} \frac{C}{N_{BTS}} < +\infty, \quad (12)$$

which is straightforwardly proved by rewriting (12) using (8)-(11) as

$$\begin{aligned} &\lim_{N_{BTS}\to+\infty} \frac{C}{N_{BTS}} \\ &= \lim_{N_{BTS}\to+\infty} E_{B,\gamma_I}\{B\log_2(1+\gamma_I)\} \\ &= E_{B,G,P}\{B\log_2(1+\frac{GP}{P_I^M + P_W})\} < +\infty. \end{aligned} \quad (13)$$

In addition to the above result, it is worth noticing that, if N_{BTS} is large enough, then (11) holds and the capacity in (8) is proportional to N_{BTS}, i.e. C is a measure with respect to N_{BTS}. This shows that Proposition 1 can be generalized to the case where the inter-cell interferences are considered. The condition on N_{BTS} such that (11) holds will be analyzed through simulation.

Remark 1. In this section, the results are presented for a single - tier network, but can be straightforwardly extended to multi - tier networks, such as presented in Appendix A.

3.3. Optimization Problem

In this section, we describe the general optimization problem of any KPI (intensive or extensive), for instance the maximization of the capacity. In the following, we denote by μ the KPI. Let Ω be the set of parameters that have an effect on the HetNet performance. Thus, Ω includes (but it is not limited to)

- The cell radius,
- The scheduler strategy,
- The number of BTSs $|B_i|$,
- The number of UEs $|U_i|$.

Furthermore, note that the KPIs themselves might be parameters of the optimization of other KPIs, e.g. one wants to optimize the capacity with respect to (wrt) a fixed power consumption. Then, the general optimization problem can be expressed as

$$\begin{aligned} &\underset{\Omega^*}{\text{opt}}\ E_\Omega\{\mu(S,\Omega)\} \\ &\text{wrt } \mathcal{C}(\Omega), \end{aligned} \quad (14)$$

where $\Omega^* \subset \Omega$, $\mathcal{C}(\Omega)$ is a set of given constraints. Solving (14) may seem to be *a priori* not tractable, due to the multivariate optimization problem. However, in most of the cases, the subset Ω^* can be reduced to a single parameter. For instance, the cell radius is linked to the transmit power, which also leads to the total number of BTS and UEs, according to a predefined density of BTSs and UEs. Furthermore, it is worth noticing that solving (14) may be simplified when KPIs can be defined as measures, such as suggested in Proposition 1. In fact, according to the properties of a measure, it should be noted that the objective function in (14) can be rewritten as

$$\underset{\Omega^*}{\text{opt}}\ E_\Omega\{\mu(S,\Omega)\} = \underset{\Omega^*}{\text{opt}} E_\Omega\{\mu(S_1,\Omega) + \mu(S_2,\Omega)\}, \quad (15)$$

where both $\mu(S1,\Omega)$ and $\mu(S2,\Omega)$ are positive values. Besides, it must be emphasized that most of the usual extensive KPIs (capacity, power consumption, scheduled bandwidth) are concave/convex functions with respect to their parameters in Ω. For instance, P and B are piecewise linear functions of the number of UEs. As a consequence, the capacity C in (1) is a linear function with respect to B, and a logarithm of the power consumption P. Since both linear ($y = ax + b$) and logarithm ($y = \log(1 + x)$) functions are concave, it can be deduced that the capacity C is concave. Since the addition of two concave functions is a concave function (keeping in mind that both

1Note that for convenience, it is usual to define r_0 as the minimum radius inside the cell, i.e. the distance from the BTS where the far field condition holds.

measures in the right side of (15) are positive), then the optimization problem in (14)-(15) is easily tractable when the KPIs are defined as measures (namely extensive variables).

Such assumptions are not valid when KPIs are intensive, since such KPIs are usually defined as ratios of measures, and (15) does not hold anymore. However, an optimal solution can be found either through numerical simulations, or through analytical derivation by reducing the number of optimization parameters which shall lead to a tractable problem, even if the KPI is not a concave/convex function. Several examples of KPIs optimization according to different parameters are given in the next two sections.

4. APPLICATION TO LTE MACRO/FEMTOCELL NETWORK

4.1. PHY Parameters of the HetNet

This section deals with the optimization of KPIs in a HetNet composed of 1 LTE macrocell and N_F LTE femtocells, such as described in Fig. 3. The femto-eNodeBs are assumed to be randomly distributed in the macrocell. Furthermore, the macro-eNodeB is a BTS featuring a tri-sector antenna, whereas the femto-eNodeB is a BTS featuring an isotropic antenna. It is supposed that the macro-eNodeBs and femto-eNodeBs transmit at two different frequencies, in order to avoid interferences between the two networks. In the proposed model, N_{UE} UEs can be connected either to the macro-eNodeB or the femto-eNodeB. Furthermore, in order to meet 5G recommendations, we propose to use an original scheduler which ensures a minimum desired throughput to each of the UEs, while limiting the resource allocation, in order to reduce the power consumption of the eNodeBs. Both macro-eNodeBs and femto-eNodeBs use the proposed scheduler, which is defined as follows. Let N_{RB}^i be the maximum number of RBs to be allocated per UE, where $i = M$ or $i = F$ may refer to the macrocell or the femtocells, respectively, then it follows that:

- If $N_{RB}^i \leq N_{RB}^{bw}/N_{UE}^i$, where nrB is the number of available resource blocks (RBs) in the bandwidth, and N_{UE}^i is the number of UEs connected to the considered macro-eNodeB or femto-eNodeB, then N_{RB}^i per UE are allocated,
- If $N_{RB}^i \geq N_{RB}^{bw}/N_{UE}^i$, then the round robin scheduler is used [26]. To summarize, the round robin scheduler allocates N_{RB}^{bw}/N_{UE}^i RBs per UE in average.

The first condition corresponds to the case where the macro- and/or femto-network are not overloaded, therefore the maximum number of can be allocated N_{RB}^i to the UEs, while reducing the power consumption since $N_{UE}^i N_{RB}^i < N_{RB}^{bw}$ (the whole spectrum resource is not used). On the other hand, the second condition corresponds to the case where the network is overloaded, and the whole spectrum resource is used. This new scheduler strategy allows the network to reduce the energy consumption, in particular in low UEs traffic periods (during the night for instance), while ensuring an equal amount of allocated RBs per UE, in average. All the variables used in the hereby developments are defined in Table 2.

4.2. Optimization of the Capacity

In this section, we provide an analysis of the achievable maximum capacity in the LTE macro/femto HetNet, according to the number of UEs per fem to cell denoted by N_{UE}^F[2], given a fixed total number of UEs in the network N_{UE}. Therefore, the set of optimization parameters Ω^* in (14) is reduced to $\{N_{UE}^F\}$, whereas is composed of all the variable described in Table 2. Furthermore, we assume that both BTS sets B_1 and B_2 use the scheduler which has been described in the previous section. For a sake of clarity, we assume that he problem is not constrained. Thus, the optimization problem of the capacity per UE can be expressed as follows:

$$\max_{N_{UE}^F} \left\{ \frac{\overbrace{N_{UE}^M C^M + N_{UE}^F N_F C^F}^{C}}{N_{UE}} \right\} = \max_{N_{UE}^F} \left\{ \frac{(N_{UE} - N_{UE}^F N_F) C^M + N_{UE}^F N_F C^F}{N_{UE}} \right\}. \quad (16)$$

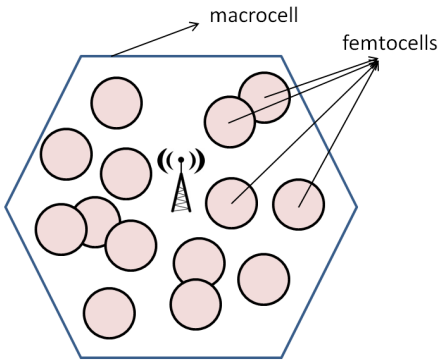

Figure 3: HetNet composed of one LTE macrocell and Np LTE femtocells.

$$C^M = R^M B_{RB} C_0^M,$$
$$C^F = R^F B_{RB} C_0^F.$$

The SE C_0^i, $i \in \{M, F\}$, can be written as follows:

$$C_0^i = E_\gamma\{\log_2(1+\gamma)\}, \quad (17)$$

where γ is the SNR, which depends on various parameters: distance from the antenna, model of shadowing and fading, antenna gain etc.

Table 2: Definition of the variables.

Variable	Definition
N_F	number of femtocells
N_{UE}^F	number of UEs/femto
N_{UE}^M	number of UEs/macro

[2] Note that N_{UE}^F differs from NUE_2 defined in Section 3 in the sense that N_{UE}^F corresponds to the number of UE per femtocell, whereas NUE_2 corresponds to the total number of UEs in all the femtocells.

N_{UE}	total number of UEs
C^M	capacity per UE in macrocell
C^F	capacity per UE in femtocell
B_{RB}	RB bandwidth
R^M	number of RBs scheduled in macrocell
R^F	number of RBs scheduled in femtocell
N_{RB}^{bw}	number of RBs in the bandwidth
N_{RB}^M	max number of RBs scheduled in macrocell
N_{RB}^F	max number of RBs scheduled in femtocell
C_0^M	SE in macrocell
C_0^F	SE in femtocell

The number of RBs scheduled in both macrocell and femtocells depends on the used scheduler. Therefore, R^M and R^F can be mathematically expressed as

$$R^M = \begin{cases} N_{RB}^M, \text{ if } N_{RB}^M \leq \dfrac{3N_{RB}^{bw}}{N_{UE} - N_{UE}^F N_F} & \text{(18a)} \\ \dfrac{3N_{RB}^{bw}}{N_{UE}^M} = \dfrac{3N_{RB}^{bw}}{N_{UE} \quad N_{UE}^F N_F}, \text{ else,} & \text{(18b)} \end{cases}$$

and

$$R^F = \begin{cases} N_{RB}^F, \text{ if } N_{RB}^F \leq \dfrac{N_{RB}^{bw}}{N_{UE}^F} & \text{(19a)} \\ \dfrac{N_{RB}^{bw}}{N_{UE}^F}, \text{ else.} & \text{(19b)} \end{cases}$$

The presence of the value 3 in (18) is due to the fact that the macrocell is a tri-sector cell, i.e. 3 x N_{RB}^{bw} RBs are available in the whole cell. Since the used scheduler leads to (18) and (19), then four cases must be considered.

$$\frac{1}{N_F}(N_{UE} \quad \frac{3N_{RB}^{bw}}{N_{RB}^M}) \leq N_{UE}^F \leq \frac{N_{RB}^{bw}}{N_{RB}^F}, \quad (20)$$

then the capacity C can be rewritten as

$$C = \frac{N_{UE}C^M + N_{UE}^F N_F (C^F \quad C^M)}{N_{UE}}. \quad (21)$$

We deduce from (21) that the variation of C with respect to N_{UE}^F depends of the sign of $C^F - C^M$. In fact, we have:

If $C^F > C^M$, then C is an increasing function, and max{C} in (16) is achieved for

$$N_{UE}^F = \left\lfloor \frac{N_{RB}^{bw}}{N_{RB}^F} \right\rfloor. \quad (22)$$

Note that we use the floor function in (22) because N_{UE}^F is an integer.

ElseIf $C^F = C^M$, then $\max\{C\} = C^M$ is achieved for any N_{UE}^F

Else $C^F < C^M$, then C is an decreasing function, and max{C} in (16) is achieved for

$$N_{UE}^F = \left\lceil \frac{1}{N_F}(N_{UE} \quad \frac{3N_{RB}^{bw}}{N_{RB}^M}) \right\rceil. \quad (23)$$

2. Case 2): from (18a) and (19b), we deduce that

$$\frac{1}{N_F}(N_{UE} \quad \frac{3N_{RB}^{bw}}{N_{RB}^M}) \leq N_{UE}^F$$

$$\frac{N_{RB}^{bw}}{N_{RB}^F} \leq N_{UE}^F$$

$$\Leftrightarrow N_{UE}^F \geq \max\left\{\frac{1}{N_F}(N_{UE} \quad \frac{3N_{RB}^{bw}}{N_{RB}^M}), \frac{N_{RB}^{bw}}{N_{RB}^F}\right\}. \quad (24)$$

We also deduce that the capacity can be rewritten as

$$C = \frac{N_{UE}C^M + N_{RB}^{bw}N_F B_{RB}C_0^F \quad N_{UE}^F N_F C^M}{N_{UE}} \quad (25)$$

Since C in (25) is a decreasing function, then we draw that max{C} in (16) is achieved for

$$N_{UE}^F = \left\lceil \max\left\{\frac{1}{N_F}(N_{UE} \quad \frac{3N_{RB}^{bw}}{N_{RB}^M}), \frac{N_{RB}^{bw}}{N_{RB}^F}\right\} \right\rceil \quad (26)$$

3. Case 3): from (18b) and (19a), we deduce that

$$N_{UE}^F \leq \min\left\{\frac{1}{N_F}(N_{UE} \quad \frac{3N_{RB}^{bw}}{N_{RB}^M}), \frac{N_{RB}^{bw}}{N_{RB}^F}\right\}, \quad (27)$$

and the capacity can be rewritten as

$$N_{UE}^F = \left\lfloor \min\left\{\frac{1}{N_F}(N_{UE} \quad \frac{3N_{RB}^{bw}}{N_{RB}^M}), \frac{N_{RB}^{bw}}{N_{RB}^F}\right\} \right\rfloor \quad (28)$$

Since C in (28) is an increasing function, then we draw that max{C} in (16) is achieved for

$$N_{UE}^F = \left\lfloor \min\left\{\frac{1}{N_F}(N_{UE} \quad \frac{3N_{RB}^{bw}}{N_{RB}^M}) \ \frac{N_{RB}^{bw}}{N_{RB}^F}\right\} \right\rfloor \quad (29)$$

4. Case 4): from (18b) and (19b), we deduce that

$$\frac{N_{RB}^{bw}}{N_{RB}^F} \leq N_{UE}^F \leq \frac{1}{N_F}(N_{UE} \quad \frac{3N_{RB}^{bw}}{N_{RB}^M}), \quad (30)$$

and the capacity C can be rewritten as

$$C = \frac{3N_{RB}^{bw}N_F B_{RB}C_0^M + N_{RB}^{bw}N_F B_{RB}C_0^F}{N_{UE}}. \quad (31)$$

3 Case 1): from (18a) and (19a), we deduce that (see Appendix B for more details)

Since C is constant, its maximum value is achieved for any N_{UE}^F UE in the interval $\left[\left\lceil \frac{N_{RB}^{bw}}{N_{RB}^F} \right\rceil, \left\lfloor \frac{1}{N_F}(N_{UE} \quad \frac{3N_{RB}^{bw}}{N_{RB}^M}) \right\rfloor\right]$.

The above results confirm that the optimization problem is easily solvable (in the considered case where the optimization is done according to the variable N_{UE}^F), since it only involves piecewise linear functions. Note that the previous developments have been carried out without any constraint, but it can be easily extended to a constrained problem, e.g. by setting a desired minimum capacity, or by limiting the number of UEs per femtocells, i.e. $N_{UE} \leq N_{UE}^{max}$ Two examples of this optimization problem are provided in Section 6. Furthermore, according to the assumption (11), the presence of interferences should not change the global behavior of the capacity versus N_{UE}^F, but the achieved capacity should be reduced. This result will be investigated through simulations.

4.3 Optimization of the Energy Efficiency

As an example of the mathematical considerations stated in Section 3.3, we can express from (5) the EE in an HetNet composed of one LTE macrocell and N_F femtocells as

$$EE = \frac{N_{UE}^M C^M + N_F N_{UE}^F C^F}{(N_{UE}^M R^M B_{RB} + N_F N_{UE}^F R^F B_{RB})(P^M + N_F P^F)}, \quad (32)$$

where P^i is the transmitted power, $i \in \{M,F\}$. The capacity per user C can be written in function of the transmitted power as

$$C^i = R^M B_{RB} \log_2\left(1 + \frac{P^i}{P^{W,I}}\right), \quad (33)$$

with $P^{W,I}$ is the interference plus noise power. It clearly appears that the EE is not a concave/convex function of any of the variables. Therefore, the maximization of such a KPI may lead to non closed-form solutions, and is still a hot topic in the field of wireless networks [27,28]. For this reason, the optimization of (32) is usually performed either through semi-analytical method [29], or by computer-aided exhaustive search, such as illustrated in Section 6. However, the main drawback of this method lies in the fact that the exhaustive search must be repeated as soon as a parameter changes, which increases the computation complexity of the problem..

5. APPLICATION TO BROADCAST-UNICAST NETWORK

5.1. PHY Parameters of the Hybrid Unicast-Broadcast Network

As described in Fig. 4, the considered hybrid unicast-broadcast network consists of two systems: a broadcast network composed of a single High Power High Tower (HPHT) station producing a broadcast signal such as DVB-NGH/T2 Lite or a modified eMBMS signal [30,31] and a unicast network composed of N^{LPLT} Low Power Low Tower (LPLT) sites producing a unicast signal according to the LTE standard. It is assumed that all LPLT sites have the same transmission parameters and coverage areas. Therefore, for a given service area, the number $N^{LPLT}$of LPLT sites is the ratio of the size of the service area to the size of a LPLT cell, which depends on the inter-site distance (ISD) between the LPLT sites. We also consider a transmission of linear TV services to N_{UE} users uniformly distributed in a given service area. The service is always available and requested by all N_{UE} users. A user requires a minimum capacity, denoted as C_{req}, to receive the proposed service. Furthermore, it is also assumed that the terminals of the users are equipped so as to be capable of switching its service reception from one network to another.

According to the general mathematical modeling of heterogeneous networks introduced in Section 3 and illustrated in Fig. 2, this hybrid unicast-broadcast network can be mathematically represented as follows:

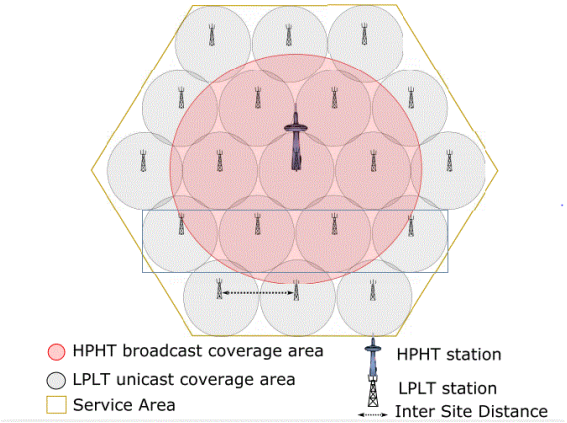

Figure 4: Hybrid unicast-broadcast network composed of one HPHT broadcast cell and N^{LPLT} LPLT unicast cell

$$S = S_{uc} \cup S_{bc}, \quad (34)$$

where $S_{uc} = B_{uc} \cup U_{uc}$ refers to the unicast system with Buc the set of N^{LPLT} BTSs and Uuc the set of users that received the service through the unicast system S_{uc} and $S_{bc} = B_{bc} \cup U_{bc}$ refers to the broadcast system with B_{bc} the set of a single HPHT station and U_{bc} the set of users that received the service through the broadcast system S_{bc}.

5.2. Optimization of the Power Consumption of the Hybrid Unicast-Broadcast Network

5.2.1. Power Consumption metric of the hybrid network

The power consumption of the broadcast network is obtained from the simplified power consumption model (6) and can be expressed as

$$P_{cons}^{bc} = P_0^{bc} + \Delta_p^{bc} P_{tx}^{bc}. \quad (35)$$

Since all subcarriers available are used for data transmission in a broadcasting system, the parameter $\rho = 1$.

In a similar way we derive from (6) the power consumption of a single LPLT cell i as follows,

$$P_{cons,i}^{uc} = P_0^{uc} + \Delta_p^{uc} P_{tx}^{uc} \rho_i^{uc}, \quad (36)$$

where

$$\rho_i^{uc} = \min\left(1, \frac{N_{RB}^i N_{UE,i}^{uc}}{N_{RB}^{max}}\right). \quad (37)$$

Observe that for the LPLT sites the parameter ρ depends on the number of users in the LPLT cell and the number N_{RB}^i of RBs that is allocated to a user, which depends on the resource allocation strategy used. Furthermore, since the traffic in the unicast cells within the coverage area of the HPHT transmitter are offloaded to the broadcast network, we consider that these LPLT cells are turned into sleep mode.

Finally the average power consumption of the hybrid network can be obtained from (35) and (36) as

$$P_{cons}^H = P_{cons}^{bc} + \sum_{i \in B_{uc}^{ON}} P_{cons,i}^{uc} + \sum_{i \in B_{uc}^{sleep}} P_{sleep}. \quad (38)$$

Recall that B_{uc} is the set of the N^{LPLT} LPLT transmitters.

5.2.2. Problem formulation

In our previous work [7], we have shown that the congestion of the hybrid network could be avoided by offloading the additional traffic data from the unicast LPLT cells of the hybrid network to the HPHT broadcast cell. We then determine, from a planning perspective, the optimal broadcast coverage radius that maximizes the overall capacity of the hybrid network for a given service area. In this paper, considering energy saving aspects, the LPLT sites within the coverage area of the HPHT broadcast cell could be turned off to save more energy when there will be no data to transmit. Therefore we hereby aim to find the optimal broadcast coverage radius that minimizes the power consumption metric of the hybrid network. The related power consumption minimization problem states

$$(P1): \quad \min_{0 \le r_{bc} \le 1} \quad P_{cons}^H(r_{bc}), \quad (39)$$

where $r_{bc} = R^{bc}/R_{max}$ is the normalized radius of the broadcast coverage area, R^{bc} and R_{max} are the radius and the maximum radius of the coverage area, respectively.

Proposed solution

Given a uniform distribution of the users in the service area, the power consumption (38) of the hybrid network is a function of the normalized broadcast coverage radius. Thus $\forall x \in [0,1]$, the objective function can be written as

$$\nu_{p1} = \frac{P_{sleep} - P_{cons,i}^{uc}}{\Delta_p^{bc} P_{tx}^{bc} r_{uc}^2}, \quad \nu_{p2} = \frac{P_{cons,i}^{uc} + P_0^{bc} r_{uc}^2}{\Delta_p^{bc} P_{tx}^{bc} r_{uc}^2}. \quad (40)$$

With

$$r_{bc}^* = \left[-\frac{2}{\alpha^{bc}} \nu_{p1}\right]^{\frac{1}{\alpha^{bc}-2}}. \quad (41)$$

Recall that P_0^{bc}, Δ_p^{bc}, P_{tx}^{bc}, $P_{cons,i}^{uc}$ and P_{sleep} are constants related to the power consumption model (6), r_{uc} is the normalized coverage radius of a unicast LPLT cell which depends on the inter site distance (ISD) and α^{bc} is the pathloss exponent for the HPHT transmitter which characterizes the propagation environment.

It can be shown from (40) that the function $f(x)$ is a convex function for all $x \in [0,1]$. Therefore the optimal broadcast coverage radius r_{bc}^* is obtained by finding the root of the derivative function $f'(x)$ where $x = r_{bc}$, which leads to

$$r_{bc}^* = \left[-\frac{2}{\alpha^{bc}} \nu_{p1}\right]^{\frac{1}{\alpha^{bc}-2}}. \quad (42)$$

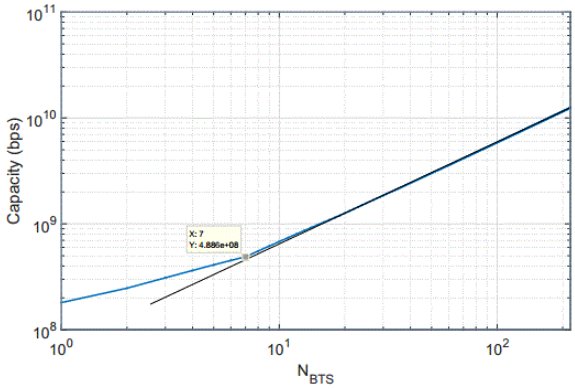

Figure 5: Capacity (8) versus N_{BTS}.

6. SIMULATIONS RESULTS

6.1. Validity of Capacity as a Measure in Presence of Interferences

The capacity (8) versus N_{BTS} in presence of inter-cell interferences has been plotted in Fig. 5. The following set of parameters have been considered: a reference distance to each of the BTSs (he. where the capacity is measured) has been set to r = 150 m, and the limit of the far field model is r_0 = 5 m. The BTSs are distributed in an hexagonal grid, the distance between two adjacent BTSs is r_k = 1000 m, the path-loss exponent is α = 3, and for the sake of simplicity, the channel gain G_k is set to 1. According to the LTE standard, the BTSs transmit at a power level of 40 W, whereas the noise power is supposed to be 10^{-5} W. The interference power depends on the number of BTSs involved in the network.

It can be observed that the capacity in (8) can be modeled as a piecewise linear function. In the case where N_{BTS} is in the range [1,7], each additional BTS is directly surrounding the BTS of interest, and therefore the induced interference from a BTS in an adjacent cell has a high level. For $N_{BTS} > 7$, the interfering BTSs are located in a further ring, which induces a lowest amount of interference compared with those located in the first ring. This leads to the break in the curve at $N_{BTS} = 7$. Thus, the capacity is approximately linear in the case where $N_{BTS} > 7$, i.e. C is proportional to N_{BTS}. As a consequence, we conclude that, in presence of inter-cell interferences, the capacity can be considered as an extensive variable from low N_{BTS} values, which illustrates the corresponding proof in Section 3.2.

6.2. Application to LTE macro/femtocell Network

6.2.1. Optimization of the Capacity

In Figs. 6 and 7, we show the different cases which have been described in Section 4. All the simulations have been obtained by using the Vienna LTE simulator [32], which has been developed in Matlab. In order to validate the results, two different sets of parameters have been considered. In Fig. 6, we used 108 UEs, a maximum of 10 RBs/UE scheduled in macrocell, 4 RBS/UE in femtocells, and 6 working femtocells, whereas in Fig. 7, we used 180 UEs, a maximum of 6 RBs/UE in macrocell, 10 RBs/UE in femtocells, and 6 working femtocells. The macro-eNodeB and femto-eNodeBs transmit with a power of 40 W and 0.1 W, respectively. Furthermore, both systems have a bandwidth of 20 MHz, corresponding to N_{RB}^{bw}= 100 available RBs. In both Figs. 6 and 7, the different plots show the capacity versus the number of UEs per femtocells. The shaded areas in Figs. 6 and 7 correspond to domains where (20), (24), (27), or (30) holds, according to the corresponding case. Further details are given below, where we show that cases.

In Fig. 6, we show that the chosen parameters lead to the following result: cases 1) and 3) hold in different ranges of N_{UE}^{F}, whereas cases 2) and 4) do not hold for any N_{UE}^{F} In Fig. 6-(a), we can observe that the shaded area corresponds to a decreasing function, according to (20) in case 1), since $C^F < C^M$. In fact, in this range of NEe, the macrocell is not overloaded, i.e. UEs in macrocell achieve their maximum of 10 scheduled RBs/UE, whereas UEs in femtocells only feature 4 scheduled RBs at the most. Then, by definition of CF and CM below (16), we deduce $C^F < C^M$.

In Fig. 6-(b) we can verify that the cases 2) and 4) lead to no solution, since (18a) and (19b) cannot hold in the same time in case 2). In fact, from (24), we deduce that $N_{UE}^{F} \geq \max\{13, 25\}$, which is inconsistent with the considered parameters as $N_{UE}^{F} \leq \frac{N_{UE}}{N_F} = 18$. Similarly, we can show that (18b) and (19b) do not hold in the same time in case 4). In addition, case 3) holds for low NFE values, since from (27) NFE < min{13, 25}, such as highlighted by the shaded area. Furthermore, it always corresponds to an increasing function, which is highlighted by the shaded area in 6-(c). Finally, we deduce from (23) and (29) that the capacity is maximized for

$$N_{UE}^{F} = \left\lceil \frac{1}{N_F}\left(N_{UE} - \frac{300}{N_{RB}^{M}}\right) \right\rceil = 13.$$

In Fig. 7, we show that the chosen parameters lead to the following result: case 1) does not hold for any NF UE value, whereas cases 1), 2), and 3) hold in different ranges of N_{UE}^{F}. Following the same approach as above, Fig. 7-(a) shows that the case 1) has no solution, since (18a) and (19a) cannot hold in the same time. In fact, $\frac{N_{RB}^{bw}}{N_{RB}^{F}} = 10$, and $\frac{1}{N_F}(N_{UE} - \frac{3N_{RB}^{bw}}{N_{RB}^{M}}) \approx 26.67$, which is inconsistent with (20).

According to the used parameters, the case 2 leads to a decreasing function (see (25)) with slope $\frac{-N_F C^M}{N_{UE}}$, which is highlighted by the shaded area on the right side of Fig. 7-(b). The case 3 leads to an increasing function for $N_{UE}^{F} \leq \min\{21.67,10\}$ from (27) and (28), which is highlighted by the shaded area on the left side of Fig. 7-(c). Furthermore, the case 4 leads to a set of solutions, where the capacity is constant and $N_{UE}^{F} \in \left[\left\lceil \frac{100}{N_{RB}^{F}} \right\rceil, \left\lfloor \frac{1}{N_F}(N_{UE} - \frac{300}{N_{RB}^{M}}) \right\rfloor\right] = [10, 20]$, achieves the maximum for any such as pointed out by the shaded area in Fig. 7-(d). Since the maximum of capacity is achieved over a set of solutions (see Fig. 7-(d)), a degree of freedom is left to the system designer (e.g. the operator) in order to choose the best solution according to another constraint such as the power consumption (or, more generally, an economical constraint). In the suggested example, it may be preferable to consider N_{UE}^{F}= 20 for consumption (and then economical) matter, since femtocells use 400 times less power than macrocells. However, the deployment and maintenance of such femto-BTSs should also be considered for a business-oriented analysis.

From Figs. 6 and 7, we notice that the use of a HetNet allows for an increase of the capacity per UE. In fact, the extremal points on the left and on the right of the figures correspond to the use of macrocell only, and the femtocells only, respectively. One can observe that these points do not achieve the maximum capacity of the HetNet, at least using the considered parameters. Moreover, it is worth noticing that the maximum achieved capacity per UE is slightly higher in Example 2 (Fig. 7) than in Example 1 (Fig. 6). This is due to the fact that N_{RB}^{F}= 10 in the Example 2 while it is only *NRFb* = 4 in Example 1. Therefore, when the 6 femtocells are not overloaded, the femto-BTSs provide 2.5 more rate in the second case than in the first case, even when more UEs are connected in Example 2 than in Example 1.

6.2.2. Optimization of the EE

In Fig. 8, we show the EE in (32) (given in bps/Hz/W) in function of femto- eNodeB power P^F (in W) and the number of femtocells N^F. P^F varies from 0 to 10 W, and N^F from 0 to 100. The other parameters in (32) have been arbitrarily set as follows: $N_{UE}^{F} = 4$, $N_{UE}^{M} C^M = 10^7$ bps, $N_{UE}^{M} R^M B_{RB} = 20$ MHz, $R^F = 10$, and $B = 18$ MHz. It can be clearly observed that the EE is not a convex function, but a global maximum is achieved over the given sets of parameters. The computer aided exhaustive search lead to the following optimal solution: {P^F=0.9, NF = 11}, but this solution strongly depends on the values of the optimization parameter and thus cannot be generalized. Furthermore, the minimum EE is achieved for P^F = 0 W and N^F = 0. Both cases correspond to the use of the macrocell only. Once again, results presented in Fig. 8, in additions to Figs. 6 and 7, show the relevance of HetNets in order to increase the capacity and the EE.

6.3. Application to Broadcast-Unicast Network

In order to validate the proposed solution which solves the optimization problem (P1), we plot the power consumption function given in (40). Then, we verify that the optimal broadcast coverage radius given by the analytical expression (42) leads to the optimal value of the power consumption

function (40). Once again, the simulations have been performed with the Vienna LTE simulator [32].

6.3.1. Simulation Settings

Let us consider a delivery of one linear service to N_{UE} = 20000 users in the service area. The users are uniformly distributed in the service area. The minimum capacity required to access the service is C_{req} = 2 Mbps. A parameter Γ, called as the SNR gap, is introduced to evaluate the effective capacity of a modulation scheme from the theoretical Shannon capacity [33]. The SNR gap is set to Γ^{bc} = 5 dB for the broadcast component and to Γ^{uc} = 3 dB for the unicast component. Then according to the service capacity requirements C_{req}, we set the minimum SNR required to receive the service through the broadcast network to γ_0^{bc} = 0 dB and the number of resource blocks (RBs) assigned to a user in a LPLT cell to N_{RB}^{i} = 2. According to the power consumption model (6), we used the power values which are summed up in Table 1. The simulation parameters are summarized in Table 3.

Table 3: Simulation settings.

Parameter	Value	
Service type	Linear contents	
Service requirement Target receiver	C_{req} = 2 Mbps	
Service area	Portable outdoor	
Distribution of users	R = 15 km	
Maximum number of users	Uniform	
	N_{UE} = 20000	
	Unicast	Broadcast
Network infrastructure	LPLT	HPHT
Network layout	hexagonal grid	single cell
Pathloss exponent	$\alpha^{uc} = 2.6$	$\alpha^{bc} = 3.1$
SNR gap (Γ)	$\Gamma^{uc} = 3$ dB	$\Gamma^{bc} = 5$ dB
Propagation losses (L_p)	8 dB	13 dB
Transmission power (EIRP)	$P_{tx}^{uc} = 1200$ W	$P_{tx}^{bc} = 1$ MW
Carrier frequency	760 MHz	690 MHz
Bandwidth	10 MHz	8 MHz
Maximum number of RBs	$N_{RB}^{max} = 50$	-
Number of RBs per user	$N_{RB}^{i} = 2$	-
Inter site distance (ISD)	750 m	-

6.3.2. Simulation Results

Fig. 9 shows the evolution of the power consumption of the hybrid network versus the coverage radius of the HPHT broadcast transmitter. In addition, Fig. 9 gives the evolution of the power consumption of the hybrid network for the case without cooperation where only one component of the hybrid network is used to deliver the service i.e. r_{bc}^{*} = 0 km and r_{bc}^{*} = 15 km. The presented results are obtained by minimizing the power consumption of the broadcast component of the hybrid network as proposed in Section 5. As shown on Fig. 9 the analytical expression of the optimal broadcast coverage radius given by (42) matches the optimal solution obtained from numerical evaluations of the power consumption function using (40). It can be also noticed that lower power consumption is achieved when the two components of the hybrid network cooperate to deliver the same service. As shown in [7] for the average capacity, the results suggest that enabling unicast and broadcast networks cooperation reduces the average power consumption which leads to a more efficient hybrid network.

7. CONCLUSION

In this paper, we modeled two-tier HetNets as σ-algebra composed of BTSs and UEs. From this model, we showed that the extensive KPIs such as capacity or power consumption can be defined as mathematical measures on this σ-algebra, whereas intensive KPIs such as EE or SE are not measures in the mathematical sense. This results has been extended to a more general scenario where SINR is considered instead of SNR. It follows that the optimization of extensive variables is much more simple than the intensive variable, especially as extensive variables are often concave/convex functions of their parameters. Several examples of optimization problems have been presented, by using two different HetNets: the LTE macro/femtocell network, and the unicast-broadcast network. The proposed developments are illustrated through simulations, which show the relevance of HetNets in order to improve the KPIs, compared with systems taken separately.

APPENDIX A: PROOF OF (11)

In order to simplify the proof, we consider a single-tier network where the BTSs are homogeneously distributed in an hexagonal grid. Thus, if we focus on a given cell, then the surrounding BTSs are sources of interferences. Note that these BTSs are distributed in rings around the cell of interest. Therefore, the number of interfering BTSs N_{BTS}— 1 can be expressed in function of the number of rings N_R and the number of BTSs per ring n_k, namely

$$N_{BTS} - 1 = \sum_{k=1}^{N_R} n_k, \tag{43}$$

where the subscript k points out the k-th ring (k = 1 corresponds to the closest ring surrounding the cell of interest). Hence P_I in (10) can be rewritten as

$$P_I = \sum_{k=1}^{N_R} G_k n_k P_r \left(\frac{r_k}{r_0}\right)^{-\alpha}, \tag{44}$$

where r_k can be approximated as a multiple of the distance between two neighbor BTSs, denoted by d_{BTS}, as $r_k \approx k d_{BTS}$. Furthermore, it can be noticed that the hexagonal grid leads to $n_k = 6k$. Then, the substitution of (44) into (11) leads to:

r_k

$$\lim_{N_{BTS}\to+\infty} P_I = \sum_{k=1}^{+\infty} G_k n_k P_r \left(\frac{r_k}{r_0}\right)^{\alpha}$$
$$= 6P_r \left(\frac{d_{BTS}}{r_0}\right)^{-\alpha} \sum_{k=1}^{+\infty} G_k k^{\alpha+1} \quad (45)$$
$$< 6P_r \left(\frac{d_{BTS}}{r_0}\right)^{-\alpha} \sum_{k=1}^{+\infty} \max_k(G_k) k^{-\alpha+1},$$

where $\max_k(G_k)$ is the maximum value of the channel gain. It should be emphasized that the series in (45) converges if $\alpha > 2$, which is the case in terrestrial propagation environment. In that case, the limit can be expressed as

$$\lim_{N_{BTS}\to+\infty} P_I \propto 6P_r \left(\frac{d_{BTS}}{r_0}\right)^{-\alpha} \zeta(\alpha-1) < +\infty, \quad (46)$$

where $\zeta(.)$ is the Riemann zeta function [34], which concludes the proof.Note that for the sake of simplicity, we limited the proof to a singletier network. However, the results presented in Section 3.2 and above can be extended to multi-tier networks, by splitting the sum according to the contributions of the different tiers. Thus, each of the tier involves different transmit power *Pr* and channel gain *Gk* values. Then, the same reasoning as above can be applied to each of the sum, which yields a result similar to (46).

APPENDIX B: PROOF OF (20), (24), (27), AND (30)

The case 1) corresponds to the scenario where neither the macrocell nor the femtocells are overloaded. From the "if" conditions in (18a) and (19a) we deduce:

$$N_{RB}^{M} \leq \frac{3N_{RB}^{bw}}{N_{UE} - N_{UE}^{F} N_F} \Leftrightarrow \frac{1}{N_F}\left(N_{UE} - \frac{3N_{RB}^{bw}}{N_{RB}^{M}}\right) \leq N_{UE}^{F}, \quad (47)$$

And

$$N_{RB}^{F} \leq \frac{N_{RB}^{bw}}{N_{UE}^{F}} \Leftrightarrow N_{UE}^{F} \leq \frac{N_{RB}^{bw}}{N_{RB}^{F}}. \quad (48)$$

The case 2) corresponds to the scenario where the macrocell is not overloaded whereas the femtocells are overloaded. From the "else" condition in (19b) we deduce:

$$N_{RB}^{F} \geq \frac{N_{RB}^{bw}}{N_{UE}^{F}} \Leftrightarrow N_{UE}^{F} \geq \frac{N_{RB}^{bw}}{N_{RB}^{F}}. \quad (49)$$

Therefore, the combination of (47) and (49) leads to (24).

The case 3) corresponds to the scenario where the femtocells are not overloaded whereas the macrocell is overloaded. From the "else" condition in (18b) we deduce:

$$N_{RB}^{M} \geq \frac{3N_{RB}^{bw}}{N_{UE} - N_{UE}^{F} N_F} \Leftrightarrow \frac{1}{N_F}\left(N_{UE} - \frac{3N_{RB}^{bw}}{N_{RB}^{M}}\right) \geq N_{UE}^{F} \quad (50)$$

Therefore, the combination of (50) and (48) leads to (27)

The case 3) corresponds to the scenario where both the macrocell and the femtocells are overloaded. Similarly as previously, the combination of (50) and (49) leads to (30).

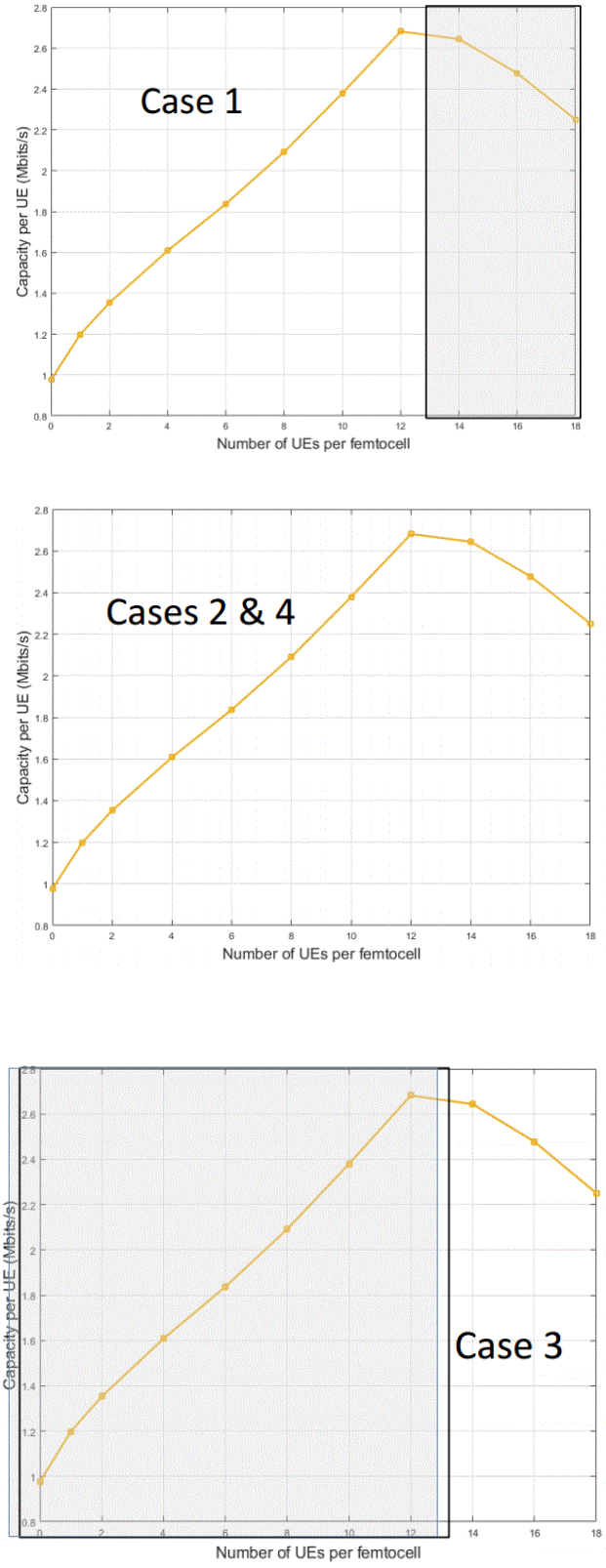

Figure 6: Optimization of the capacity in LTE heterogeneous network, using 108 UEs, 10 RBs in macrocell, 4 RBS in femtocells, and 6 working femtocells.

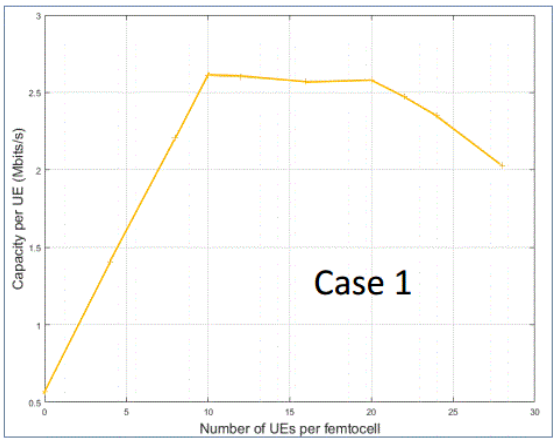

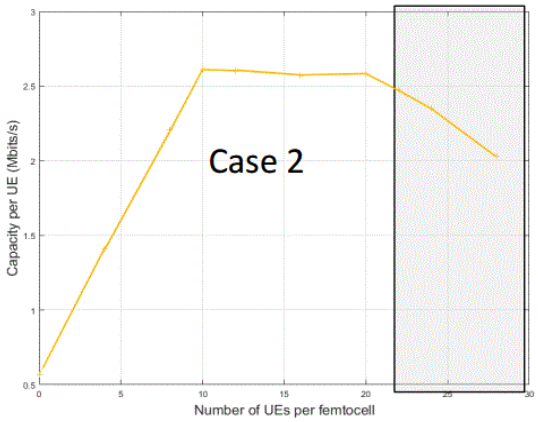

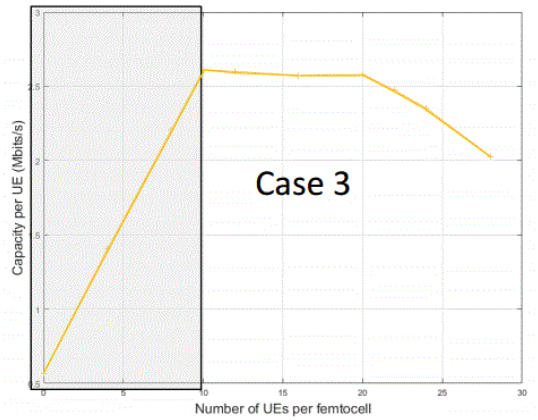

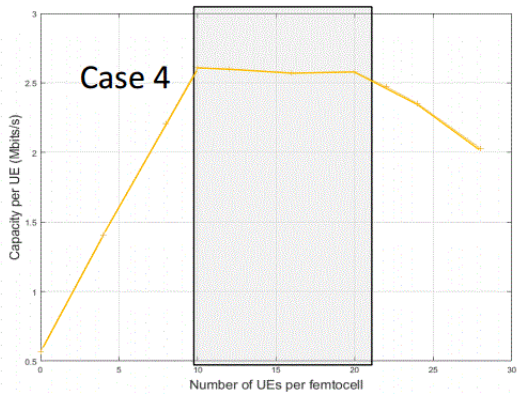

Figure 7: Optimization of the capacity in LTE heterogeneous network, using 180 UEs, 6RBs in macro-cell, 10 RBS infemtocells, and 6 working femtocells.

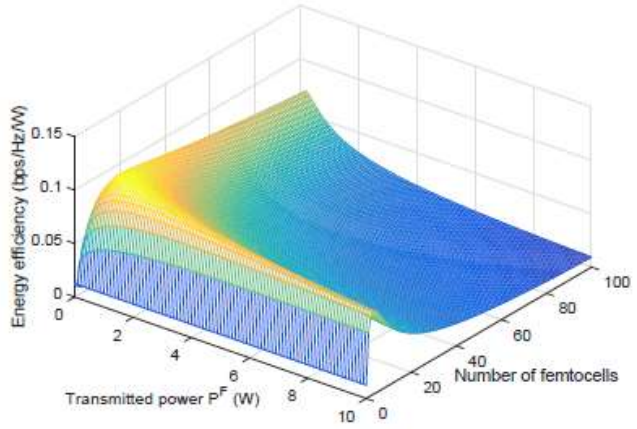

Figure 8: Energy efficiency (bps/Hz/W) versus PF and NF.

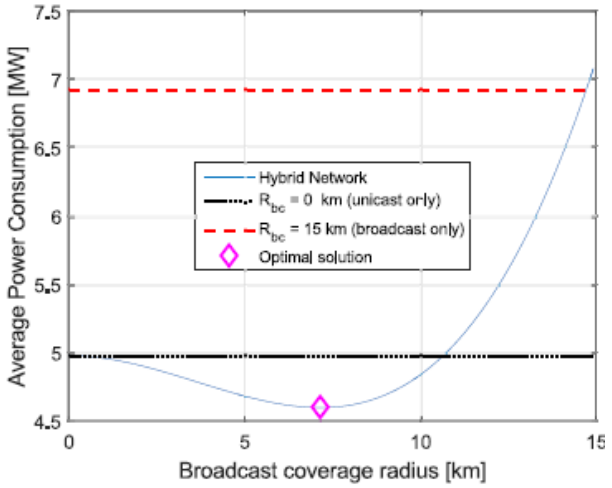

Figure 9: Power consumption of the hybrid network vs broadcast coverage radius; NUE = 20000; NRB = 2.

LIST OF ABBREVIATIONS

3/4/5G	Third/fourth/fifth generation of mobile phone mobile communication technology standards
AWGN	Additive White Gaussian Noise
BS	Base Station
BTS	Base Transceiver Station
CSMA-CA	Carrier Sense Multiple Access with Collision Avoidance
DVB-T2	Digital Video Broadcasting-Terrestrial 2nd generation
EE	Energy Efficiency
EMBMS	Evolved Multimedia Broadcast Multicast Service
eNodeB	Evolved Node B: base station of the mobile networks based on LTE or LTE-A
HetNet	Heterogeneous Network
HPHT	High Power High Tower
KPI	Key Performance Indicator
LPLT	Low Power Low Tower

LTE	Long Term Evolution
NGH	Next Generation Handheld
PHY	Physical layer
RB	Resource Block: in LTE, a block of 12 adjacent subcarriers of 15 kHz each
SE	Spectral Efficiency
SINR	Signal-to-Interference plus Noise Ratio
SNR	Signal-to-Noise Ratio
UE	User Equipment

CONFLICT OF INTEREST

The author declares that there are no conflicts of interest.

REFERENCES

[1]. A. Ghosh, R. Ratasuk, B. Mondal. LTE-advanced: next-generation wireless broadband technology, IEEE Wireless Communications 2010; 17 (3): 10 - 22.

[2]. A. Ghosh, N. Mangalvedhe, R. Ratasuk, B. et al. Novlan, Heterogeneous Cellular Networks: From Theory to Practice, IEEE Communications Magazine 2012; 50 (6): 54 - 64.

[3]. M. Gerasimenko, N. Himayat, S.-P. Yeh, S. Talwar, S. Andreev, Y. Koucheryavy. Characterizing Performance of Load-Aware Network Selection in Multi-Radio (WiFi/LTE) Heterogeneous Networks, in: proc. of Globecom'13, Atlanta, GA, 2013, 397 - 402.

[4]. C. Heuck. An Analytical Approach for Performance Evaluation of Hybrid (Broadcast/Mobile) Networks, IEEE Transactions on Broadcasting 2010; 1(56): 8 - 18.

[5]. X. Gu, X. Deng, Q. Li, L. Zhang, W. Li. Capacity Analysis and Optimization in Heterogeneous Network with Adaptive Cell Range Control, Hindawi International Journal of Antennas and Propagation 2014 ; 1 - 10.

[6]. A. Martinez-Vargas, A. Andrade. Deployment analysis and optimization of heterogeneous networks under the spectrum underlay strategy, EURASIP Journal on Wireless Communications and Networking 2015; 55: 1 - 15.

[7]. P. A. Fam, S. Paquelet, M. Crussiere, J.-F. Helard, P. Bretillon. Optimal capacity of hybrid unicast-broadcast networks for mobile TV services, in: proc. of IEEE International Symposium on Broadband Multimedia Systems and Broadcasting (BMSB'16), Nara, Japan, 2016.

[8]. P. A. Fam, S. Paquelet, M. Crussiere, J.-F. Helard, P. Bretillon. Analytical Derivation and Optimization of a Hybrid Unicast-Broadcast Network for Linear Services, IEEE Transactions on Broadcasting 2016; 62(4): 890-902. dOI: 10.1109/TBC.2016.2593403.

[9]. N. Cornillet, M. Crussiere, J.-F. Helard. Optimization of the energy efficiency of a hybrid broadcast/unicast network, in: proc. of WCNC Workshop (WCNC'13), Shanghai, China, 2013.

[10]. Y. S. Soh, T. Q. S. Quek, M. Kountouris, H. Shin. Energy Efficient Heterogeneous Cellular Networks, IEEE Journal on Selected Areas in Communications 2013; 31 (5): 840 - 850.

[11]. R. Q. Hu, Y. Qian. An Energy Efficient and Spectrum Efficient Wireless Heterogeneous Network Framework for 5G Systems, IEEE Communications Magazine 2014; 52 (5):94 - 101.

[12]. J. Tang, D. K. C. So, E. Alsusa, K. A. Hamdi, A. Shojaeifard. Resource Allocation for Energy Efficiency Optimization in Heterogeneous Networks, IEEE Journal on Selected Areas in Communications 2015; 33 (10) : 2104 - 17.

[13]. P. Lin, Y. Chen, Q. Zhang. Macro-femto heterogeneous network deployment and management: from business models to technical solutions, IEEE Wireless Communications 2011; 18 (3): 64 - 70.

[14]. A. Goldsmith, Wireless Communications, Standford University.

[15]. S. Choudhury, J. D. Gibson. Ergodic capacity, outage capacity, and information transmission over Rayleigh fading channels, in: proc. of the Information Theory and Applications Workshop, 2007.

[16]. M. K. Simon, M.-S. Alouini, Digital Communication over Fading Channels, John Wiley & Sons, 2000; 2: 15 - 30.

[17]. N. D. Chatzidiamantis, H. G. Sandalidisy, G. K. Karagiannidis, S. A. Kotsopoulosz. On the Inverse-Gaussian Shadowing, in: proc. of IC-CIT'11, Aqaba, Jordan, 2011; 142 - 146.

[18]. B. Selim, O. Alhussein, S. Muhaidat, G. K. Karagiannidis, J. Liang. Modeling and Analysis of Wireless Channels via the Mixture of Gaussian Distribution, IEEE Transactions on Vehicular technology.

[19]. Y.-N. R. Li, et al., Energy efficient small cell operation under ultra dense cloud radio access networks, in: Globecom Workshops (GC Wkshps) 2014; 1120-5.

[20]. G. Auer, et al., Energy efficiency analysis of the reference systems, areas of improvements and target breakdown, INFSO-ICT-247733 EARTH (Dec. 2010).

[21]. F. Heliot, M. A. Imran, R. Tafazolli. On the Energy Efficiency-Spectral Efficiency Trade-off over the MIMO Rayleigh Fading Channel, IEEE Transactions on Communications 2012; 60 (5) :1345 - 56.

[22]. F. Richter, A. J. Fehske, G. Fettweis. Energy Efficiency Aspects of Base Station Deployment Strategies for Cellular Networks, in: proc. of VTC'09-Fall, Anchorage, AK, 2009; 1 - 5.

[23]. S. Cui, A. J. Goldsmith, A. Bahai, Energy-efficiency of mimo and cooperative mimo techniques in sensor networks, IEEE Journal on Selected Areas in Communications 22 (6).

[24]. C. Desset, et al., Flexible power modeling of LTE base stations, in: IEEE Wireless Communications and Networking Conference (WCNC) 2012; 2858-2862.

[25]. M. Le Bellac, F. Mortessagne, G. G. Batrouni, Equilibrium and Non-Equilibrium Statistical Thermodynamics, Cambridge University Press 2004; 3: 95 - 174.

[26]. E. L. Hahne. Round-Robin Scheduling and Window Flow Control for Max-Min Fairness in Data Networks, IEEE Journal on Selected Areas in Communications 1991; 9 (7): 1024 - 1039.

[27]. L. Deng, Y. Rui, P. Cheng, J. Zhang, Q. T. Zhang, M. Li, A Unified Energy Efficiency and Spectral Efficiency Tradeoff Metric in Wireless Networks, IEEE Communications Letters 2013;17 (1): 55 - 58.

[28]. D. Feng, C. Jiang, G. Lim, L. J. Cimini, G. Feng, G. Y. Li. A Survey of Energy-Efficient Wireless Communications, IEEE Communications Surveys and Tutorials 2013; 15 (1): 167 - 178.

[29]. C. T. Kelley, Iterative Methods for Optimization, Society for Industrial and Applied Mathematics Philadelphia, 1999.

[30]. D. Rother, al., A Software Defined Radio based implementation of the Tower Overlay over LTE-A+ system, in: Broadband Multimedia Systems and Broadcasting (BMSB), 2014 IEEE International Symposium on, IEEE 2014: 1-6.

[31]. M. Crussiere, al., A Unified Broadcast Layer for Horizon 2020 Delivery of Multimedia Services, IEEE Transactions on Broadcasting 60 (2) (2014) 193-207. doi:10.1109/TBC.2014.2315764.

[32]. C. Mehlfuhrer, J. C. Ikuno, M. Simko, S. Schwarz, M. Wrulich, M. Rupp. The Vienna LTE simulators - Enabling reproducibility in wireless communications research, EURASIP Journal on Applied Signal Processing 2011; (29) :1 - 14.

[33]. J. M. Cioffi, et al., Mmse decision-feedback equalizers and coding. ii. coding results, IEEE Trans. Commun 1995: 43 (10). 2595-2604. doi:10.1109/26.469440.

[34]. M. Abramowitz, I. Stegun, Handbook of Mathematical Functions with Formulas, Graphs, and Mathematical Tables, Dover, Ney York, 1970, Ch. 6.